Assessing and Improving the TMT LGSF Thermal Performance with CFD Modeling

Lianqi Wang

Assessing and Improving the TMT LGSF Thermal Performance with CFD Modeling

Lianqi Wang*[a], Konstantinos Vogiatzis[a], Melissa Trubey[a], Ben Irarrazaval[a], Corinne Boyer[a],
[a]TMT International Observatory, Pasadena, CA 91124, USA. *lianqiw@tmt.org

ABSTRACT

In order to maximize the laser guide star adaptive optics system's performance, the laser launch system needs to minimize the projected spot size at the sodium layer by both minimizing the output laser beam wavefront error and focusing the beam correctly in the sky. However, with the continuously changing thermal environment, including radiation cooling and intermittent laser heating of the lenses, it is not trivial to achieve the two goals. We have recently carried out unsteady thermal computational fluid dynamics (CFD) modeling of the laser guide star facility (LGSF) for TMT to assess its thermal behavior. The temperature distribution of the lenses and lens mounts are fed into the Code V optical design software to assess the induced focus and wavefront error, while the temperature gradient of the air is used to determine the tube seeing. The optical baffle length, thermal resistance between the lenses and lens mounts, as well as dry air flushing, have been treated as parameters and optimized as a result. In this paper, we will present the findings.

Keywords: Adaptive optics, laser guide star facility, tube seeing, TMT.

1. INTRODUCTION

The TMT Laser Guide Star Facility (LGSF) [1] beam transfer optics (BTO) [Figure 1] is mainly composed of the following components:

1. A relay lens and multiple automated fold mirrors for each laser beam, which transfer the laser beam from the laser platform below the primary mirror to the telescope top end while compensating for the gravity and thermal flexure errors as well as relaying the laser beam waist to an asterism mirror at the top end.
2. An Asterism Generator that formats laser beams into a selectable asterism while providing individual beam pointing and center adjustments and jitter compensation.
3. A Launch Telescope Assembly that expand the beam size to 240 mm $1/e^2$ diameter, de-rotate and project onto the sky while providing focus and pointing adjustments.

The Relay lens and Collimator spacing are automated to provide focus adjustments. The Laser Launch Telescope (LLT) can pivot on its supporting axis to provide telescope flexure compensation. The fold mirror inside the LLT can provide medium bandwidth jitter and flexure compensation.

There are additional components providing automated control functions:

1. A low power module for each beam to reduce the power level for alignment.
2. Pre-alignment cameras measuring beam position using scattered light from mirrors or lenses.
3. A Diagnostic System Wavefront Sensor (DSWFS) providing pointing/centering/power/wavefront error for all beams simultaneously.
4. A beam dump and mirror providing top end shutter while enables alignment and calibration without propagating to the sky.

The total throughput is estimated to be ~83% with 14 fold mirrors, 6 lenses, and 2 quarter wave plates. The wavefront error budget allows 40/76 nm in high/low order modes.

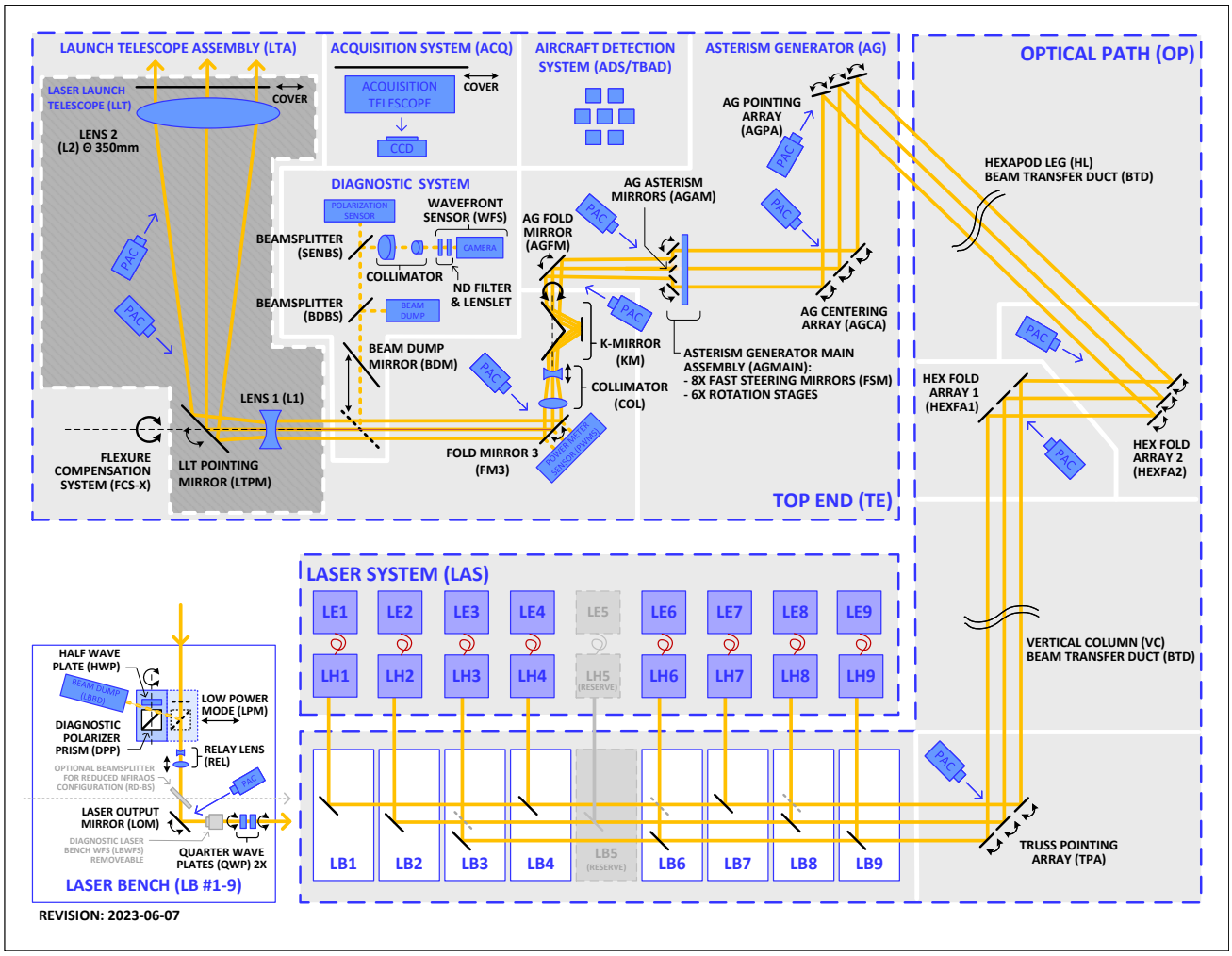

Figure 1 LGSF layout

Figure 2 shows the Laser propagation for two beams with the three sets of powered optics (without the fold mirrors). Two different Relay Lens prescriptions are used to compensate for the propagation distance variation.

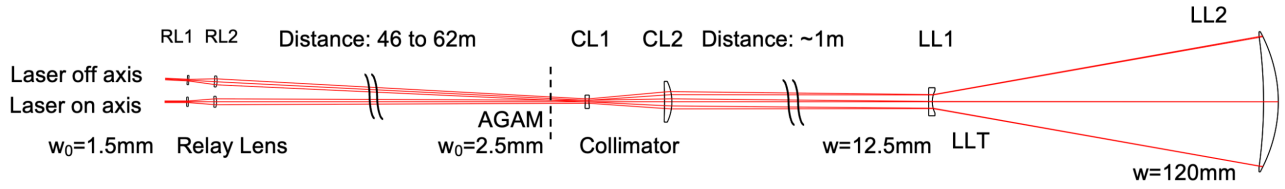

Figure 2 Laser propagation for two beams without the fold mirrors.

Figure 3 shows the LTA and Diagnostics System optical ray trace. This part of the system is designed together in geometric optics mode. The AGAMs form the entrance field while the LLT exit lens forms the pupil. The Diagnostic System Collimator reimages the pupil onto a lenslet array with 8×8 subapertures.

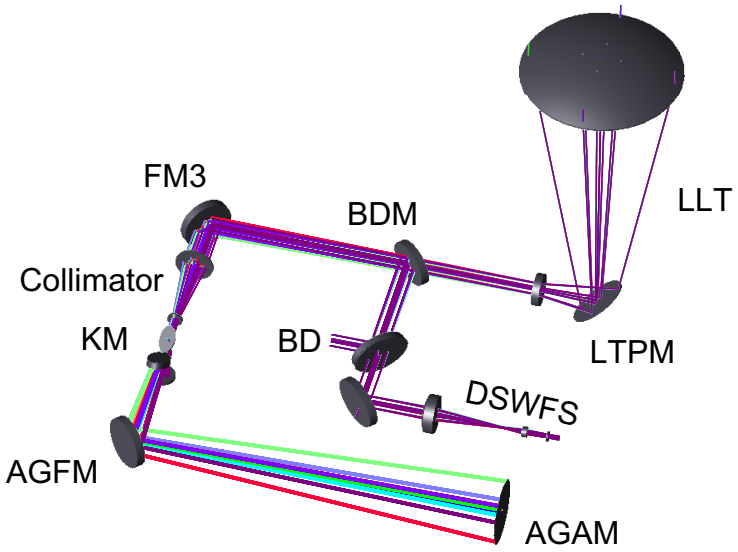

Figure 3 LTA and Diagnostics System Optical Raytrace

Each of the powered optics (RL, COL, LLT) is athermalized by lens material selection allowing focus dependence matching the spacing material (invar-36, with CTE=1.2e-6/K).

The continuously changing thermal environment, such as convection, radiation, conduction and intermittent laser heating of the mirrors and lenses have been modeled with the latest mechanical design using Computational Fluid Dynamics (CFD) to assess and optimize the performance [2]. The CFD analysis and optical modeling results are presented below.

2. CFD SETUP

The LGSF is divided in several standalone conjugate heat transfer models at the laser bench (LB, below the laser head), along the beam transfer ducts, at the top end, and for the LLT. Each conjugate heat transfer model solves for the temperature of all structural and optical components, as well as the temperature and flow pattern of the air inside the LGSF; heat exchange occurs at the solid/solid and solid/air contact interfaces. The Boussinesq buoyancy model for air is employed. The simulations are performed sequentially; the exit air temperature record of the LB array is used as input in the beam transfer ducts model and so on. The duration of the simulation (nighttime) is 11 hours during which the zenith angle is kept fixed at 30° which results in average buoyancy conditions between the two limiting cases (0° or 65°). The simulation time step is 300 seconds.

The inputs include material and thermal properties, ambient temperature profile on exterior surfaces, convective heat transfer coefficients on exterior surfaces, laser power absorption for optics, power dissipation from actuators etc. An additional “sky” component is placed at the observatory enclosure aperture level and kept at an effective temperature of 260K is used for radiative coupling with the exterior component surfaces. The effective temperature can be a function of time representing variations due to zenith angle.

The output include time and space records of component temperatures, time, and space records of air refractive index along the LGSF optical path. MATLAB post-processors convert the temperature fields into beam OPDs.

3. CFD RESULTS

Figure 4 shows the temperature distribution after 11 hours of laser heating and heat exchange with the environment for the original LLT design with or without a sky baffle. With the sky baffle, the temperature of the big lens facing the sky is significantly warmer than the ambient while without the sky baffle, the opposite is true. We have reduced the baffle to 1/6

of this original length so that the temperature is closer to the ambient. Figure 5 shows the updated and simplified LLT design (to improve its athermal performance) with reduced baffle.

The lens mount thermal resistance and dry air flushing have also been optimized as a result. The larger lens of the LLT now features a non-conductive lens mount to reduce the thermal gradient within the lens, while the remaining lenses all have conductive lens mounts to reduce and stabilize their overall temperatures. The airflow has been increased/optimized to reduce the tube thermal seeing.

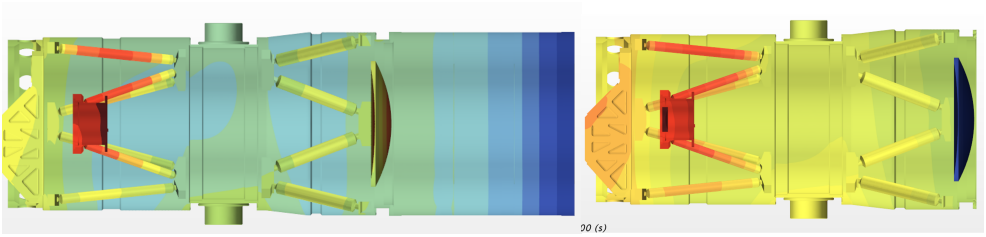

Figure 4 End of night temperature distribution of the original LLT design with or without the sky baffle.

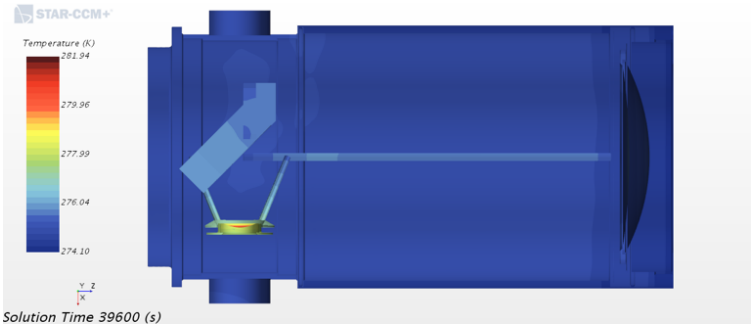

Figure 5 End of night temperature distribution of the updated LLT design with a shortened sky baffle.

Figure 6 shows the temperature distribution at end of the night for the Relay Lens and Collimator. The center of each lens is heated by laser beam to significantly above the ambient. The temperature cross sections are shown in Figure 7.

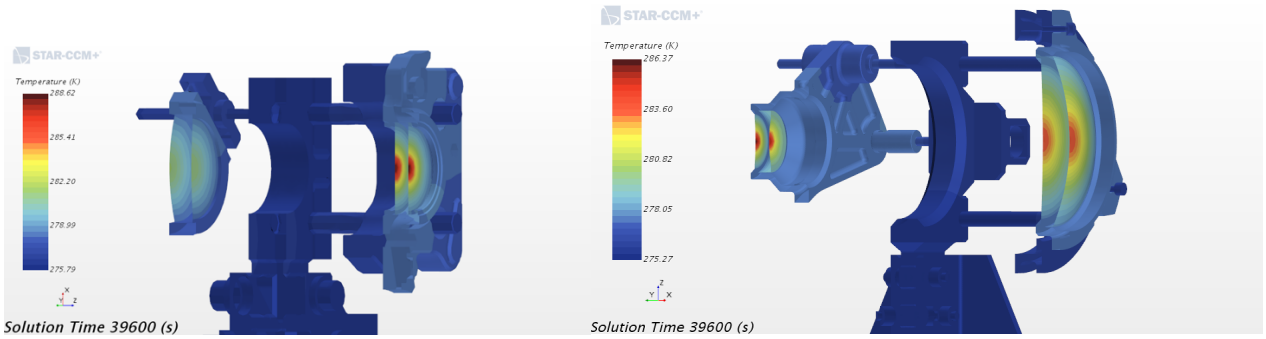

Figure 6 End of night temperature distribution of the Relay Lens (left) and the Collimator (right).

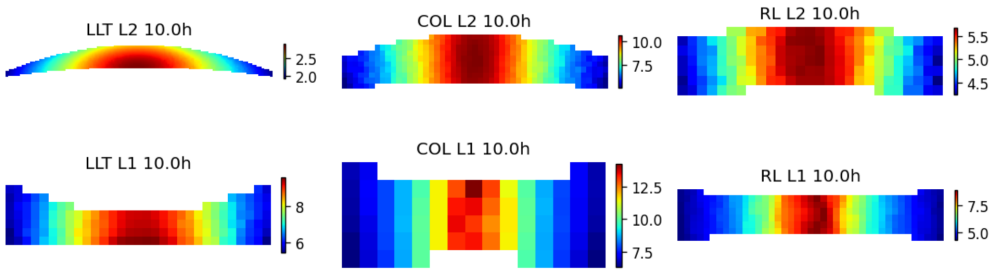

Figure 7 Cross-section temperatures of the LLT, Collimator, and Relay Lenses after 10 hours of continuous Laser heating.

Finally, the lens temperature profiles are fed into Code V using thermal gradient operator to compute the focus and wavefront error. The results are shown in Figure 8. The focus removed wavefront errors are negligible. The Relay Lens and Collimator focus error stabilizes quickly after laser propagation and may be controlled using a shutter open time based LUT. The excessive and slowly varying focus error of the LLT may require feedback control based on spot size measurements of the LGS WFS subaperture but is not expected to impact the LGS acquisition process.

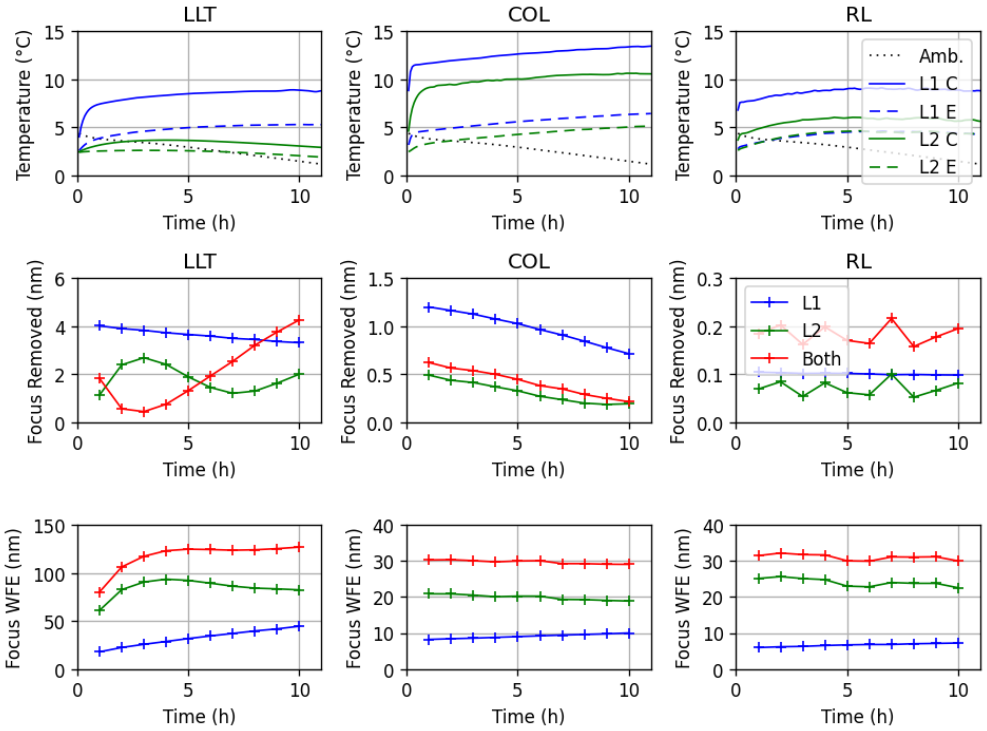

Figure 8 Time history of the ambient and lens temperatures at the Center and Edge (top panels), Focus (bottom panels), and focus removed Wavefront Error (middle panels) for each of the powered optics.

Figure 9 shows a time snapshot of the air refractive index gradient within the various enclosures. They are converted into OPDs along the optical path of a laser beam. The tip/tilt, tip/tilt removed low order and high order wavefront error are then computed for each time step with results shown in Figure 10. The tip/tilt values have been scaled to on sky pointing error based on the beam magnification ratio. The wavefront error is predominantly in low order modes and has been incorporated into the LGSF wavefront error budget. The beam jitter is mostly semi-static and the medium to high frequency content is negligible compared to the uplink turbulence.

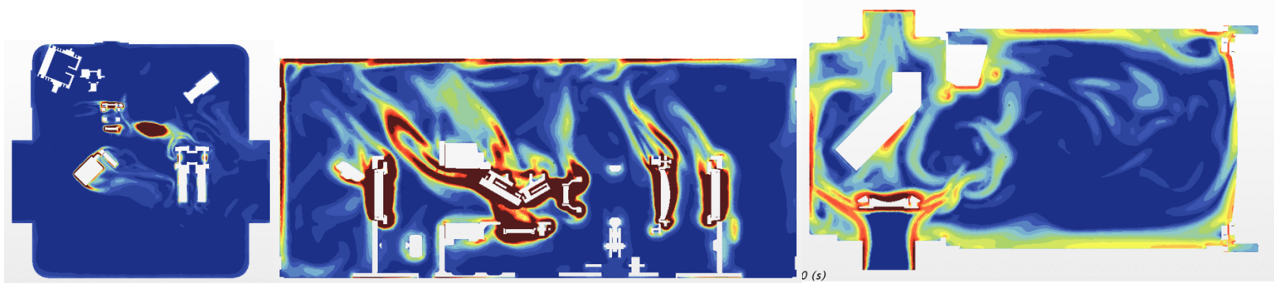

Figure 9 A snapshot of the air refractive index gradient (cross section) in the Laser Bench (Left), K-mirror and Collimator (Middle), and LLT (Right).

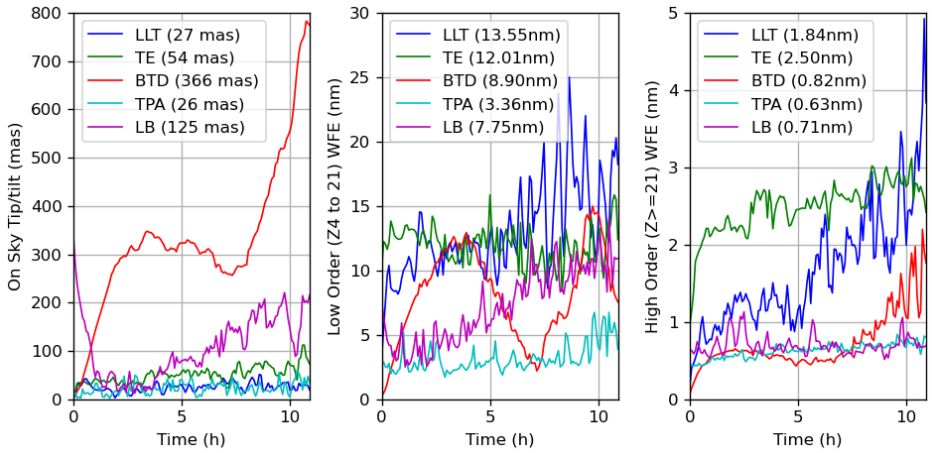

Figure 10 The thermal seeing at the Laser Bench (LB), TPA, beam transfer ducts (BTD), the top end (TE) and the LLT with time and spatial RMS shown in the legend.

4. CONCLUSION

We have assessed the LGSF transient thermal performance with CFD simulations and optical modeling. Two major findings are with the transient focus error and tube seeing.

The transient focus error of the Relay Lens will need to be calibrated using PAC at the top end for each beam and maybe controlled using a LUT based on the shutter open time. The focus error of the Collimator can be calibrated using the DSWFS while the focus error of the LLT cannot be directly measured and need to be optimized in closed loop by minimizing the time averaged spot size as measured by the LGS WFS subaperture due to its slow convergence with time and dependence on the ambient and sky temperatures.

The tube seeing are dominated by slowly varying tip/tilt and low order aberrations and do not pose a significant risk to the performance.

REFERENCES

[1] Melissa Trubey, Corinne Boyer, Angelic Ebbers, Ben Irarrazaval, John Miles, Fernando Santoro, Konstantinos Vogiatzis, Lianqi Wang, "TMT Laser Guide Star Facility Preliminary Design", AO4ELT7 (2023)

[2] Konstantinos Vogiatzis, Corinne Boyer, et al. Aero-thermal simulations of the TMT Laser Guide Star Facility, SPIE (2014).